EVALUATION OF POSSIBILITIES AND PERSPECTIVES OF APPLICATION OF NANOMATERIAL HARD COATINGS

MAGDALENA KOPERNIK, MACIEJ PIETRZYK

Department of Modelling and Information Technology, Faculty of Metals Engineering and Industrial Computer Science,
AGH – University of Science and Technology, Kraków, Poland

Abstract

The paper is a review of the research on applications and testing of the nanomaterial hard coatings. The processing techniques for these materials and their main applications are presented first. The second part of the review is focused on the main objective of this work, which is numerical modelling of deformation of the nanomaterial hard coatings. Various approaches to this problem and main difficulties are discussed. Three main tests, which are used to identify the material parameters in the constitutive models, are described. The second part of the paper deals with the results of simulations performed by the Authors. Results of the finite element simulations of the nano-indentation test for multi-layer coating are presented and the predictive capabilities of the model are confirmed. The model will be further implemented into the inverse software for the considered tests.

Key words: Nanomaterial hard coating, nano indentation test, nano impact test, finite element modelling, inverse analysis

1. INTRODUCTION

Nowadays nanomaterials are often manufactured as functionally graded materials (FGM) and have their characteristic features. FGMs have innovative properties and/or functions that cannot be achieved by conventional homogeneous materials. In their simplest structure, they consist of one material on one side, a second material on the other, and an intermediate layer whose structure, composition and morphology vary smoothly from one material to the other at the micron level (Kawasaki and Watanabe, 1997). Thus, the main feature of FGMs is gradual variation of properties with position.

This definition do not comprise single-phase materials, however, such possibility is open for intermetallics based on γ-titanium aluminide (Kieback et al., 2003). The amount of $α_2$ and γ-phases in these materials after heat treatment and the type of microstructure (lamellar, globular and duplex), that can be

distinguished by slight variations of composition, allow to classify them as FGMs.

FGMs as unique composite materials have applications in structural materials, that can endure high temperature exposure with wear or corrosion resistance. Applications can be extended from structural to electrical, chemical, optical, nuclear and biomedical areas. Thermal barrier coating systems for land-based gas turbines (Kravchuk et al., 1994; Kobel'skij et al., 1999) and more-efficient aircraft engines are the most demanding applications of FGMs. The expected property of these systems is high-temperature resistance from one side and good mechanical performance on the other side. For example, if FGMs are to be used to separate regions of high and low temperature, they may be composed of pure ceramic, at the hotter end, and pure metal at the cooler end. The NiCrAlY + YSZ (Kravchuk et al., 1999) systems are the most widely used materials for this purpose.

Functionally graded materials are recently

widely manufactured and applied in several specific technologies. Experimental tests on FGMs are carried out in the best equipped laboratories. However, these materials are still very demanding and difficult in experiments, and there are still unsolved, experimental problems. These problems can be successfully solved using computer aided interpretation of measurements. Therefore, the problem of modelling of FGMs is investigated by the authors.

Perspective development of FGMs and scarce research on modelling of these materials inspired authors to investigate this field. The particular objectives of this paper are twofold. The first is the review of research on FGMs. The second is the investigation of the possibility of application of the inverse analysis to determination mechanical properties of investigated FGMs. Formulating the direct problem model for the inverse analysis is part of this objective.

2. FUNCTIONALLY GRADED MATERIALS

2.1. Example of a technical problem

The FGM coating development arose from the fact that the design of more advanced, yet conventional thermal barriers, turned out to be a complex task. Initially, the FGM concept was developed only as method of managing residual stresses and elimination of sharp interfaces encountered in the conventional systems. However, graded regions composed of ceramic and metallic constituents became unstable upon exposure to oxidative atmosphere. Thus, a more effective approach consisting of incorporated additional oxygen barrier layer (Lee et al., 1996) in the coating structure, was adopted. The role of such layer, that is to be functionally graded, is to retard oxygen transport to the surface and provide a good mechanical compliance between two layers (Fig. 1).

The most important role of FGM layers in thermal barrier systems is to minimise and/or release residual stresses (Ravichandran, 1995) through the proper variation in composition/microstructure.

2.2. Material properties

The optimal properties of FGMs are derived by taking advantage of diversified and spatially dependant properties of their components. Thus, the
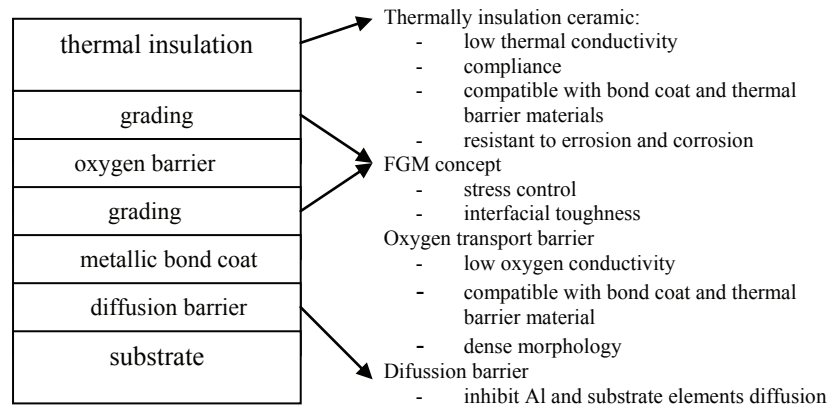

Fig. 1. The criteria for thermal barrier system composed of FGMs (Lee, 1996)

FGMs design requires a detailed knowledge of a number of material properties at high temperatures, including (Yang et al., 2003) thermal conductivity λ, elastic modulus E, shear modulus μ, Poisson ratio ν, linear thermal expansion coefficient α, oxygen diffusivity and remaining mechanical properties (microhardness, strength, toughness, creep). These properties influence the thermal and mechanical response of the system, and are used for residual stresses calculations. Then properties of candidate for coating materials are selected.

2.3. Processing techniques for FGMs

In the synthesis, FGM is fabricated by a variety of fabricating processes, according to the pre-designed gradient structure. Fabricating processes (Table 1) are roughly classified into three groups (Kawasaki and Watanabe, 1997): gaseous, solid and liquid processes.

Gaseous processes allow to prepare directly thin films or plates while controlling gas flow rates and/or temperature. The powder metallurgical process is one of the most viable routes for FGM, in which a wide range of composition control and microstructure variation are allowed, along with the shape forming freeform. This process allows also to obtain a bulk material as well as thin coating layers. The self propagating high temperature synthesis (SHS) is characterised by easy sintering of the bulk material in a relatively short time.

2.3.1. Powder metallurgy (PM)

Overview of manufacturing methods for FGMs is treated here generally, especially in powder metallurgy, because is not the subject of this paper.

Table 1. Fabrication processes of FGM (Kawasaki and Watanabe, 1997)

Phase	Process	Material combination
Gas	CVD	SiC/C, SiC/TiC, TiC/CC[a]/C-C[b] composite, C/ceramics
Gas	Ion plating	TiN/Ti, TiC/Ti, ZrO_2/Cu, C/Cr
Gas	Plasma spraying	YSZ[c]/NiCrAlY, YSZ/NiCr
Gas	Ion mixing	diamond/WC, YSZ/Cu
Liquid	Electrodeposition	Ni/Cu
Liquid	Plasma spraying	YSZ/NiCrAlY, YSZ/Ni-Cr
Liquid	Eutectic reaction	$Si/ZrSi_2$
Solid	SHS	TiB_2/Cu, TiB_2/Ni, TiC/Ni, $MoSi_2$-SiC/TiAl, ZrO_2/Ni PZT/Ni, PZT/Nb
Solid	Powder metallurgy	YSZ/SS304[d], YSZ/Mo, YSZ/Nb, SiC/AlN/Mo
Solid	Diffusion	Si_3N_4/Ni, W/Cu, Ni/Al.

[a] CC – carbon composite, [b] C – C – carbon-carbon, [c] YSZ – Yttria Stabilized Zirconia,
[d] SS304 – carbon steel

Powder metallurgy (PM) or ceramic technology route for processing of materials and engineering parts include powder production, powder processing, forming operations, sintering or pressure assisted hot consolidation (Kieback et al., 2003). The following types of gradients can be obtained by the powder metallurgy route: porosity and pore-size gradients, gradients in chemical composition of single phase materials, gradients of the volume content of phases and grain size gradients in two or multiphase materials. Formation of graded powder compact is composed of deposition of layers of powder mixtures with stepwise change, continuous dry deposition of layers, sheet lamination, wet powder spraying, slurry dipping and solid freeform process. Deposition of powder with continuous changes in the mixture can be done in centrifugal powder forming (CPF) and impeller-dry blending, gravity sedimentation, centrifugal sedimentation, electrophoretic deposition, pressure filtration/vacuum slip casting and sintering.

Gradient formation can be conveniently achieved by transport processes in the molten state and subsequent consolidation. Melt processing is widespread for FGMs containing a metal as one

Table 2. Overview of processing methods for FGMs (Kieback et al., 2003)

Process	Variability of transition function ♦ (Z.M. Yang, 2003)	Layer thickness[a]	Versatility of phase content	Type of FGM	Versatility in component shape
Powder stacking	Very good	M, L	Very good	Bulk	Moderate
Sheet lamination	Very good	T, M[b]	Very good	Bulk	Moderate
Wet powder spraying	Very good	UT, T[b]	Very good	Bulk[c]	Moderate
Slurry dipping	Very good	UT, T[b]	Very good	Coating	Good
Jet solidification	Very good	M, L	Very good	Bulk	Very good
Sedimentation/ centrifuging	Good	C	Very good	Bulk	Poor
Filtration/slip casting	Very good	C	Very good	Bulk[c]	Good
Laser cladding	Very good	M	Very good	Bulk, Coating	Very good
Thermal spraying	Very good	T	Very good	Coating, Bulk	Good
Diffusion	Moderate	C	Very good	Joint, Coating	Good
Directed solidification	Moderate	C	Moderate	Bulk	Poor
Electrochemical gradation	Moderate	C	Good	Bulk[c]	Good
Foaming of polymers	Moderate	C	Good	Bulk	Good
PVD[d], CVD[e]	Very good	C	Very good	Coating	Moderate

[a] L: large (>1 mm); M: medium (100-1000 μm); T: thin(10-100 μm); UT: very thin (<10 μm); C: continuous, [b] Depending on available powder size, [c] Maximum thickness is limited, [d] PVD – physical vapour deposition, [e] CVD – chemical vapour deposition
♦ In a FGM the properties change gradually with position. The property gradient in the material is caused by a position-dependent chemical composition, microstructure or atomic order. In the case of a position-dependent chemical composition the gradient can be defined by the so-called transition function (Yang et al., 2003) $c_i(x, y, z)$, which describes the concentration of the component c_i as a function of the position.

constituent. Melt processing is composed of centrifugal casting, sedimentation casting, controlled mould filling, directional solidification, infiltration processing and reactive infiltration.

2.3.2. Processing of polymers – basis of FGMs

In polymers (Kieback et al., 2003), like in other materials, compositional and microstructural gradients are intended to allow an optimum combination of component properties, for example: weight, surface hardness, wear resistance, impact resistance and toughness. Polymers with a porosity gradient, so-called polyurethane integral skin foams provide high impact strength at low weight and have been used since long for instrument panels or head rests in cars. Graded polymers that have been processed so far include graded fiber composites, graded interpenetrating polymer networks, graded biodegradable polyesters and graded index polymer fibers and microlenses. Comparing to ceramic or metal based systems, the knowledge about processing methods for polymer FGMs is limited. Thus, some important processing methods for polymer FGMs are described in this chapter and particular attention is given to the methods used in the polymers processing program, which will be called "priority program". This program is composed of projects and is focused on achievements in the field of FGM processing techniques, especially in the field of graded polymer processing, which is described by Kieback et al. (2003).

In polymer composites, a gradient of the reinforcement can be introduced by centrifuging prior to polymerisation. This method was studied in detail by Klingshirn (mentioned by Kieback et al., 2003). Two resins were used as matrix materials, while SiC particles, aramide particles, glass fibers and carbon fibers were used as filler materials. Rings and tubes with a gradient in filler content were produced by centrifuging a dispersion of particles in a resin prior to hardening. The wear resistance of thermosetting polymers was improved by the addition of the hard filler particles or fibers.

It was demonstrated (mentioned by Kieback et al., 2003) that the gradient in filler content leads to a corresponding gradient in microhardness and wear resistance. Long-fiber reinforced polymers with graded fiber composition or orientation can be produced by lamination techniques. In a "priority program" project a gradient was introduced also in the matrix material. Polycyanurate resins were used as a matrix material. Since the neat polycyanurate is too brittle for many structural applications, it was modified by a rubber modifier. Higher modifier contents improve the toughness, but the good high-temperature stability of neat polycyanurate and the resistance against water absorption are reduced. The idea of the project (mentioned in a "priority program") was thus to optimise the properties of a component by a gradient in modifier content, in addition to gradients in fiber density and orientation which are already used in lightweight components.

The gradient was achieved by hot press lamination of a stack of glass fiber containing differently modified resins. Since the resins are redistributed between the layers during molding, it was necessary to determine the resulting gradient at the end of the process. This was done by dynamic mechanical analysis (DMA) which proved that a smooth gradient was established during molding.

If polymers (mentioned by Kieback et al., 2003) develop distinctly different microstructures at different processing temperatures, it is possible to introduce property gradients by applying a temperature gradient during processing. Such an effect was used in a project (mentioned in a "priority program") aiming at the development of a polymeric impact protection material consisting of a single component. Sintered fiber materials were selected as candidates because they have high energy absorption potential.

The properties of the final product depend strongly on the temperature, at which the fibers are sintered together. Low sintering temperatures lead to an anisotropic microstructure in which the aligned fibers are still well discernible. High sintering temperatures lead to a compact, isotropic material. Components with either of these microstructures have poor moderate impact resistance.

The anisotropic material fractures by delamination between the fibers, so that small objects can penetrate through the material between the fibers and the high strength of the fibers cannot be used for the absorption of impact energy. On the other hand, the isotropic microstructure, per se, has low impact resistance. The idea of the project (mentioned in a "priority program", Kieback et al., 2003) was to introduce a microstructural gradient by applying a temperature gradient during sintering with the goal to improve the impact properties of the component. For one of the test materials, the liquid-crystalline copolyester Vectran®, the idea was successful.

2.4. Biomedical applications

Biomaterial is defined as a bioactive material used in a medical device, intended to interact with biological systems, restore functions of natural living tissues and organs in the body. Many biomaterials, such as metals, ceramics, polymers and composites, have been tested for the use in the body. However, few have achieved human clinical application. Functional gradient is one of characteristic feature of living tissue.

Bio-inspired materials open new perspectives for manufacturing implants for bone replacement. Different routes for new implant materials are shown using the principle of functional gradation. An artificial biomaterial for knee joint replacement (Pompe et al., 2003) was developed by building a graded structure consisting of ultra-high molecular weight polyethylene (UHMWPE) fibre reinforced by high-density polyethylene combined with a surface of UHMWPE. The growth of titanium implants into hard tissue can be improved by depositing a graded biopolymer coating of fibronectin, collagen types I and III with a gradation, derived from the mechanisms occurring during healing in vivo. Functionally graded porous hydroxyapatite (HAP) ceramics can be produced using alternative routes, e.g. sintering of laminated structures of HAP tapes filled with polymer spheres or combining biodegradable polyesters such as polylactide, polylactide-co-glycolide and polyglycolide, with carbonated nanocrystalline hydroxyapatite. HAP-collagen I scaffold is an appropriate material for in vitro growth of bone. The scaffold has to be functionally graded in order to create an optimised mechanical behavior as well as the improvement of the cell growth.

Hydroxyapatite (HA) coated Ti-6Al-4V (M. Inagaki et al., 2003) prevents the corrosion of the underlying material and HA has the ability to cause growth of the bone up to the implant. HA being a bioactive material combined with non-toxicity and bioinert Ti-6Al-4V is a promising implant for orthopaedics applications, which provides an implant that is biocompatible, light and stable.

Cementum – dentin junction CDJ (Ho et al., 2004) is classified as a functionally graded dental tissue. This region contributes to a gradual variation in hardness and chemical composition from cementum to dentin and forms a material with good biomechanical characteristics over a width of approximately 80 to 200 mm.

2.5. Design and modelling studies applied to FGM

2.5.1. Design

A design is intended to take advantage of certain desirable features of each of the constituent phases. For example, if the FGM is to be used to separate regions of high and low temperature, it may consist of pure ceramic, at the hotter end, because of the ceramic's better resistance to the higher temperatures. In contrast, the cooler end may be pure metal because of its better mechanical and heat-transfer properties. Major problems in the design of FGM (aside of material selection) (Markworth et al., 1995), are:

− Determining of the optimum spatial dependence for the composition. Composition profile best accomplishes the intended purpose of the material, while maintaining other thermal, physical and mechanical properties within limits that ensure acceptable performance.

− Predicting the characteristics of FGMs, for a given composition profile, during fabrication and under inservice conditions.

− The composition of FGMs can vary widely. It means that a variety of fundamentally different microstructures can exist along the graded direction. The thermophysical properties, which are generally dependent on the microstructure, will vary with position within the material. A realistic model must appropriately account for these variations.

2.5.2. Modelling

Two principal topics connected with modelling are covered in the literature. The first is macroscopic versus micromechanical analysis. Models of microstructure dependent thermophysical properties will be discussed below as the second topic.

Macroscopic versus micromechanical analyses. There are two ways of characterization of FGMs' response to mechanical and thermal loads under various loading conditions: continuous and discrete models. Different aspect of the system were accounted for, namely: geometry, deformation and fracture mechanics, including elastic and plastic contributions to crack propagation. The continuous approach is based upon the assumption of continuous spatial changes of material properties. Continuous model gives correct solution to such problems as

elastic deformation in the ceramic-rich side and plastic deformation in the metal-rich side of the analyzed systems in the case when the scale of the problem is greater than the grain sizes of their phase constituents. The same observation pertains to damage initiation that starts from microstructural imperfections, like voids or cracks, having size greater than the grain size. The continuous model was formulated based upon the "rule of mixture" (Markworth et al., 1995).

The strongly heterogeneous microstructure is likely, at least possible, to cause locally concentrated tailed residual stresses during thermal or mechanical loading. These locally concentrated stresses, especially those high in tension, may initiate small cracks and voids. The development of these small-scale failures may lead to large-scale failures and result in fracture of the whole structure.

In the discrete micromechanics model, the ceramic grains are treated to be elastically deformed as the typical ceramic materials. The metal grains undergo thermo-elastoplastic, finite deformation, and are treated using the crystal plasticity theory. The results show that the local stress concentration at the grain size level is significant.

The continuous model. The model geometry consists of three layers: the ceramic layer is on the one side, the metal layer is on the other side and the FGM (precisely interlayer or functionally graded layer) is sandwiched between them. A model system is described below. It is chosen the metal to be Ni and the ceramic to be Al_2O_3. The FGM is, therefore, Ni/Al_2O_3 FGM (Dao et al., 1997). The variable x is defined as the relative distance from ceramic - FGM interface, i.e. $x = 0$ stands for the ceramic - FGM interface and $x = 1$ stands for the FGM - metal interface. For the continuous model for the FGM, the effective material properties are assumed to follow the rule of mixture:

$$A(x) = V_{Metal}(x)A_{Metal} + V_{Ceramic}(x)A_{Ceramic} \qquad (1)$$

where A stands for either the elastic constants, E (Young's modulus) and v (Poisson's ratio), or the thermal expansion coefficient α; $V_{Metal}(x)$ and $V_{Ceramic}(x)$ are the volume fractions of metal and ceramic, respectively, at the position x.

The simplified material property form overlooks the interactions of the two material phases at the microscopic level, so it leads to an approximate solution. The more accurate material property variation formed at the macroscopic level requires a better understanding of FGM microstructure and its de-

formation. The continuous model gives correct solutions to elastic deformation in the ceramic-rich side and plastic deformation in the metal-rich side. In above model system is obtained the elastic solution. In the implementation, the FGM layer is divided into 30 micro-layers and the material properties of each micro-layer are taken to be constant. A finite element method is used for the purpose of examining its accuracy for FGMs.

The discrete micromechanics model. A computation micromechanics model for FGMs is using the crystal plasticity theory. The model geometry for a FGM consisting of the metallic and ceramic grains randomly distributed within it. The ceramic grains are treated to be elastically deformed as the typical ceramic materials; the metal grains undergo thermo-elastoplastic, finite deformation, and are treated using crystal plasticity theory. The macroscopic material properties obtained by statistical processing of the random distribution of the metal and ceramic grains vary continuously along the thickness direction, and give their desired variation forms. Having these assumptions and many others (presented by Dao et al., 1997) we find out that the total deformation gradient is decomposed into plastic (F^P), thermal (F^θ), and lattice (F^*) attributions.

Mentioned above the single crystal constitutive theory (McHugh et al., 1993) has been implemented into finite element codes, using tangent method (Pierce et al., 1983). The analysis of the results of the calculation (made for the continuous and the discrete micromechanics model on Ni/Al_2O_3 FGM example, introduced above) allowed the statement that the optimal FGM microstructure should be built upon porous material.

Dense-compacted microstructure is proved for local stress concentrations. The micro-fracturing behavior of FGMs is sensitive to grain size of ceramic components. Fine grain sized microstructure is preferred to improve the resistance of FGMs against cracking. As a final conclusion, it is stated that local residual stresses play an important role in the failure initiation. Therefore, local microstructural features should be considered in modeling FGMs.

Finite and boundary element methods. The thermal and mechanical response of FGMs can by calculated by solving equations for non-stationary heat transfer and for thermal stresses. The residual stresses have a substantial effect on coating properties. They contribute to deformation of coated elements and spallation. The nature of residual stresses influences various types of coating properties, such as

bond strength, resistance to thermal cyclic and corrosion resistance. Both, finite FEM and boundary element methods (BEM) are used for calculations of thermal and mechanical response of the FGMs, when temperature and stress distributions are calculated for the purpose of FGMs design and performance optimalization. The FEM is the most effective in dealing with complicated nature of thermal and mechanical response of FGMs, examples are given in (Bansal and Pindera, 2003; Carneiro et al., 2004). The elastic stresses in materials subjected to mechanical loading are determined using the finite element method (Cheng and Batra, 2000), which subsequent stages of the solution are as in (Carneiro et al., 2004).***Models for thermophysical properties.*** The effective thermophysical properties of heterogeneous materials are related to the microstructure of the material. Generally, one can distinguish three causes of continuous properties variations (Markworth et al., 1995), namely:

− Position-dependent chemical composition variations,

− Gradual microstructure variations,
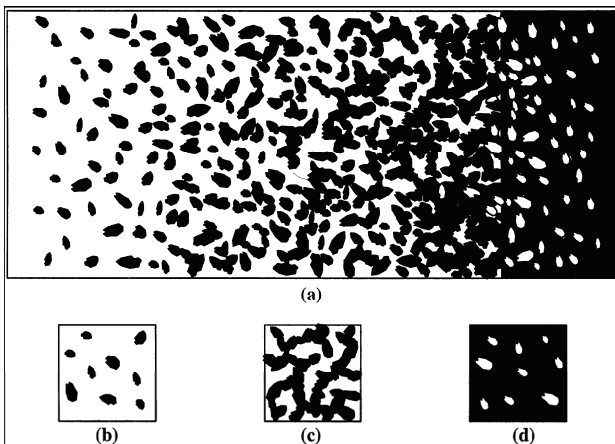
− Gradual atomic order variations.

Fig. 2. (a) schematic representation of the variation in FGM microstructure; (b) and (d) typical microstructure at small volume fractions of the two materials, (c) typical microstructure at comparable volume fractions of the two materials (Dao et al., 1997)

The most complicated case to deal with quantitatively is when microstructural variations have to be exploited in order to obtain a required spatial distribution of properties. To manage this situation, three basic types of geometric morphologies (compare Fig.2b-d) associated with the distribution of phases inside a two-phase material were defined, namely:

− Dispersed grain structure (eg. Fig. 2b) – material for which the volume fraction of one phase is low, and is discretely and randomly distributed within the host phase. It is also characteristic of a material, for which the volume fraction of the dispersed phase is somewhat higher, but the phase remains discretely and uniformly dispersed.

− Aggregated grain structure (eg. Fig. 2c) – the volume fraction of the minor phase is increased to the point that it is no longer discrete, but is aggregated in the form of clusters of definite size.

− Percolation - like cluster structure (eg. Fig. 2d) – as the volume fraction of the minor phase is increased still further, it reaches a critical value, called the percolation threshold, at which it is interconnected to such an extent that there exists a continuous random cluster, as well as small aggregated clusters.

The most important material properties that must be known for numerical predictions of thermomechanical response of thermal barrier systems comprise: thermal conductivity, elastic module, linear thermal expansion coefficient, oxygen diffusivity and mechanical properties (strength, toughness, creep).

The knowledge of thermophysical properties of thermal barrier components, as well as their spatial distribution in functionally graded layer allows the calculation of temperature and stress distribution in the system during the fabrication stage and at service.

Models for specific thermoplastic properties of a heterogeneous material are based on some kind of microstructure - dependent mixture rule (Markworth et al., 1995). Additional considerations of mixture rules for thermophysical properties are given by (Hirano et al., 1988), who related the pertinent rule for various properties (thermal conductivity, coefficient of thermal expansion, elastic modulus and shear modulus) to the nature of the microstructure. Analytical and numerical models for mechanical and thermal properties of plasma sprayed ceramic coatings are described in (Argyris et al., 1994; Kesler et al., 1998; Kohr and Gu, 2000). Mechanical behavior (Argyris et al., 1994) was studied using computer generated microstructure of lamellar ceramic coating. Thermal conductivity was calculated as affected by the presence pores. The pore volume occurred as the most influencing parameter reducing the thermal conductivity.

Works connected to FGMs concern in damage mechanism analysis and modeling under thermal-mechanical cyclic loading are reflected in (Butcher

et al., 1999; Delale and Erdogan, 1983; Eischen, 1987; Erdogan, 1995; Erdogan and Wu, 1997; Gu and Asaro, 1997; Gu and Dao, 1999; Jin and Batra, 1996; Parameswaran and Shukla, 1998; Thogo et al., 1996), (Kesler et al., 1998; Kirchoff, 2004).

3. TiN/Ti/POLYURETHANE

TiN/Ti/polyurethane, a functionally graded nanomaterial can be used in artificial heart as a building material in chambers and valves. Heart aortic valve prosthesis (Nałęcz, 2001) is made up of three identical leaflets (Li et al., 2001), which have constant thickness along whole surface. Valve leaflet material can have polyurethane substrate (Ghista and Reul, 1983) and TiN nanocoating (Lackner, 2005a). Leaflet's material consists of three basic layers: polyurethane/Ti/TiN and two interlayers: polyurethane/Ti and Ti/TiN. Such material is called FGM (Major et al., 2003), because it has gradual variation of properties with position. Intermediate layer structure (Major et al., 2004b), composition and morphology vary smoothly from one material to the other at the nanometer level (Major et al., 2004a).

Titanium nitride (TiN) coatings have proved their efficiency in increasing the lifetime of cutting tool (Major et al., 2004a). The tests undertaken showed that wear was reduced, the TiN friction coefficient (Major, 2005) was low and the TiN presented good chemical stability.

The titanium nitride coatings are fabricated by PLD (Lackner et al., 2002) method. A Nd:YAG laser operating at the fundamental harmonics is used to deposit the TiN on non-metallic (polyurethane) substrates by ablation of high purity titanium nitride target. In the PLD technique a pulsed laser beam is focussed onto a target in order to evaporate its surface layers under vacuum or low pressure process gas conditions.

The vaporised material consisting of atoms, ions and atomic clusters is then deposited onto the substrate. The outstanding advantage of this technique is the possibility to deposit coatings of very high chemical purity and adhesion to various substrate materials at room temperature. Furthermore, high rate film growth on surface areas situated perpendicular to the targets surface is also possible by using a low-pressure process gas. The application of reactive process gases leads to the opportunity of varying the film stoichiometry in a wide range.

Deposition of the TiN at ambient conditions on polyurethane substrate revealed that the uniform thin layer and diameter of crystallite was related closely to the thickness of the deposited layer. An evident grain growth is visible. It tends to increase together with an increase of the layer thickness. Examination of the TiN layers fabricated at room temperature on polyurethane substrate showed a correlation between the increase of grain size and of the layer thickness.

An increase of the layer thickness was achieved by using a higher number of laser shots while the other deposition parameters were constant. Morphology observation of the cross-section of broken samples revealed a good adhesion which was inferred from the smooth interface layer/substrate, and more evidently from the change of concentration of titanium on line scan. The TiN layers deposited on polyurethane are of pseudodiffusive character (Lackner, 2005a), which can be inferred from the diffusive shape in surface region of the substrate proved by the EDX line scan of Ti through the thickness (Fig. 4.b).

3.1. Tribological properties

TiN has excellent tribological properties and a golden colour. The tribological process (Matthews et al., 1998) in a contact between the two surfaces includes mechanical and tribochemical changes as well as material transfer (Holmberg et al., 2000). Tribological contact mechanisms are: macromechanical, material transfer, micromechanical, tribochemical and nanomechanical contact (Holmberg et al., 1998).

Thin hard coatings on a soft substrate generate lower stresses in the coating and at the coating/substrate interface compared with thick hard coatings with the same deflection. A multilayer coating with alternate hard and soft layers can allow deflection to occur under load without yielding of the hard layers. They effectively slide over each other, with shear occurring in the soft layer. The pattern of shear is illustrated by the line through the film, which was initially straight in the unloaded condition (Holmberg et al, 1998).

Structure of TiN coatings on metallic titanium are examined (Oleś, 1998) using X-ray diffraction (XRD), atomic force microscopy (AFM) (Oleś, 1998), transmission electron microscopy (TEM) and were performed to study surface morphology (AFM) and microstructure of the cross section (TEM) as well as crystallographic texture (Rauschenbach and Gerlach, 2000) and residual stresses (XRD) (Schwarzer, 2005). Three materials were under ex-

COMPUTER METHODS IN MATERIALS SCIENCE

amination i.e. not treated surface of the titanium sheet just after rolling with average roughness 0.9229 μm, mechanically ground, roughness 0.6409 μm and mechanically polished roughness 0.3483 μm.The influence of the crystallographic texture in the substrate and the deposited layer was discussed. The textures in the substrate in all cases were different and could influence the texture of the layer. In the first case when the TiN was deposited on as rolled substrate with 0.9229 μm roughness the maxima of the substrate and the layer were in the same position. The character of both pole figures was axial and well generated. In the second case the orientation was strong in spite of the high disturbance of the orientation of the substrate and no generation was observed. The texture character of the TiN layer deposited on mechanically polished substrate (roughness 0.3483 μm) was axial, similar to the substrate. Inheritance was good. TiN films are deposited in on-axis and off-axis target-substrate arrangement (Lackner et al., 2004a) and have different properties, as well as microstrucures. In the room-temperature PLD grown crystalline coatings nanoclustered surfaces are evident (Lackner, 2005b) – both in on-axis and of-axis coatings.

Nanostructure coating models are widely characterized by (Dobrzański, 2002). The Structure Zone Model (SZM) made by Thornton is often used for sputtered coatings. Only very small columns are obtained for on-axis deposited TiN-films, which correspond to the zone-T structure (Thornton, 1974).

The most uniform and isotropic stress distribution was observed for the layer deposited on the substrate with the lowest roughness and the axial type of the stress distribution. Variation of the compressive residual stress in the range of 4 to 10 GPa measured in the TiN coating was stated in respect to the surface state.Thin foil examination on TEM revealed a blurred character between the nanocrystalline deposited TiN coating to the polycrystalline metallic titanium. Electron diffraction pattern achieved by selected area diffraction technique revealed nanocrystalline structure of the TiN deposited layer on the metallic titanium, which could be associated with the uniform distribution of the particles. In the samples with Ti substrate the interlayer had a blurred character from the TiN coating to the substrate, which could confirm good adhesion. The development of tribological coatings of new generation seems to be expected in functionally gradient materials.Appearing high value of stress in monolayer tribological coatings leads in many cases to micro-cracks formation. The elimination of this disadvantage can be expected from the stress reduction due to interlayer application of super-elastic material, which separates super-hard layers and could moreover block cracks propagation during exploitation.

The surface morphology, analyzed by atomic force microscopy (AFM) of the Cr and Ti based multilayer coatings revealed a high uniformity in both cases. A mean roughness was in order of hundreds of micrometer which verified the PLD as the method producing high quality surfaces. Layers produced by pulsed laser deposition technique were characterized by high, compressive residual stress 12 and 4.5 GPa for Ti/TiN/Ti/TiN and Cr/CrN/Cr/CrCN, respectively (Major, 2005). The recent results obtained on materials with different numbers of layers based on Ti, presented that residual stress decreases with increasing number of layers.

The tribological wear tests (Lackner et al., 2004b) were performed using the pin-on-disc method with application of 9.81N load and the obtained results showed the friction coefficient 0.2 for Ti/TiN/Ti/TiN system. Moreover, the wearing process of super-hard TiN and compensation Ti layers could be examined by variation of the friction coefficient. Wear tests for TiN were also made by (Gu and Lin, 1996a, 1996b; Gu et al., 1996), (Shouterden et al., 1995) and fretting test in aqueous solution is shown in (Wu et al., 1996).

TiN layers will be potentially used for the implantable biomaterials (Czarnowska et al., 1999). When blood comes in contact with biomaterial surface it is necessary to guarantee a suitable degree of the roughness, which is required to form natural biolayer formed by blood proteins. The PLD method allows to control the surface roughness, what ensues from the current experience and achieved results. A search for materials, which in miniature elements could be used in medical equipment, was a goal of the research on multilayer tribological materials of new generation (Kustosz et al., 2004). To guarantee a non-failure service of elements at difficult exploitation conditions is a new challenge for researchers. Application of the PLD method for fabrication of the multilayer tribological system seems to be helpful.

ChronoThaneP (Lackner, 2005a) – the TiN/Ti/PU system's substrate is thermoplastic polyurethane elastomer. Polymers are examined, for example according to ASTM standards and such data is available in material specifications. Material properties like: tensile strength (at yield and at break), tensile

modulus (for elastomers, this is stress at a given % strain), strain, elongation and percent elongation at yield, elongation and percent elongation at break, flexural strength, flexural stress at specified strain levels, flexural modulus, vicat softening temperature are given by producers. Theoretical explanation of polymers physical behavior is shown in (Przygocki and Włochowicz, 2001). Polymer descriptions mentioned above include: ASTM D-2240, ASTM D-412, ASTM D-624, ASTM D-1525, ASTM D-790 standards (Table 3) (http://www.ptli.com).

Table 3. ChronoThaneP
(http://cardiotech-inc.com/products/chronothanep.asp).

Durometer (Shore) ASTM-2240	80A
Tensile Strength ASTM D-412	35,163 MPa
Elongation ASTM D-412	550%
Modulus @ 100% Elongation	5,86 MPa
Modulus @ 300% Elongation	12,066 MPa
Tear Strength Die "C" ASTM D-624	2,896 MPa
Vicat Softening ASTM D-1525	185°F
Flexural Modulus ASTM D-790	103,421 MPa

3.2. Mechanical properties

TiN/Ti/PU mechanical properties are used in simulations performed in the present work. Each material layer has its own properties and they are set into programme. Experimentally obtained property values for TiN (Cai and Bangert, 1996; Wang and Bangert, 1993) are used by Major and Lacki (2005) in the thin film modeling behavior. TiN is an elastoplastic bilinear material (Saliklis et al., 2003) and Ti as well as PU are elastic media. Nonlinear behavior of elastic-plastic and elastic materials is decribed by Gere and Timoshenko (1984) using stress-strain diagrams (Morawiecki et al., 1977). Theoretical fundamentals for material models are shown in (Bathe, 2004; Hansel and Spittel, 1978), as well as in the FORGE® V.2.4 materials database (2004), The FORGE® V.3.6 materials database (2005). These material models are based on (Bathe and Montans, 2004; Drysdale and Zak, 1985): a) the Huber-Mises yield condition, b) an associated flow rule using the Huber-Mises yield function, c) an isotropic or kinematic, bilinear or multilinear, hardening rule.

Such composite material is mainly considered to be hard coating on soft substrate, but also sandwich structure (Schärer and Rohner, 2003). Typical for thin films is wrinkling phenomenon (Fig. 3.), experimentally proved by Basu et al. (2005). Using relations (Volynskii et al., 1999; Volynskii et al., 2000; Landau and Lifshitz, 1986; Stoney, 1909), simple compression FEA simulation was made by Lackner (2005a) and complete numerical experiment was shown by Kopernik and Pietrzyk (2006). According to selection of set FEA elements wrinkling like in thin films and composite sandwich structure (Gdoutos et al., 2003) occurs in work Kopernik and Pietrzyk (2006).
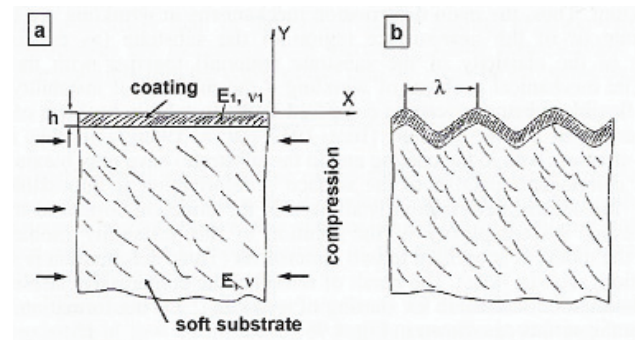

Fig. 3. Schematic drawing of the wrinkling phenomenon: (a) Initially smooth coated polymer surface, (b) Release of compressive stresses in the substrate and coating result in wrinkling of the compound (Lackner, 2005a)

Results obtained by Kopernik and Pietrzyk (2006) can be compared to basic features of constructed composites mechanics (Ochelski, 2004). By Ochelski (2004) boundary and scale effects are theoretically risen, but multilayer behavior depends on number of layers and it isn't clearly precised. In that way it cannot be compared to Kopernik and Pietrzyk (2006) multilayer's jump test results, which is done for multilayers consisting of 3 and 7 period Ti/TiN layers deposited on PU substrate.

The concepts of the discrete element method is presented for impact resistance analysis of composites (Mohammadi et al., 2002). The method is capable of analyzing the progressive fracturing and fragmentation behavior, as well as potential post-cracking interactions caused by the newly created crack sides and segments. A special remeshing method has been developed to geometrically model an individual crack by splitting the element, separating the failed node, creating new nodes and dividing the neighbouring elements to preserve the compatibility conditions. The method has proved to be an efficient approach for impact analysis of composites undergoing progressive delamination and cracking.

3.3. Interlayers

There is an interlayer occurrence between TiN/Ti and Ti/PU (Fig. 4. and Fig. 6.). These layers

presence is confirmed by experiments (Lackner et al., 2004a), (Lackner, 2005c).
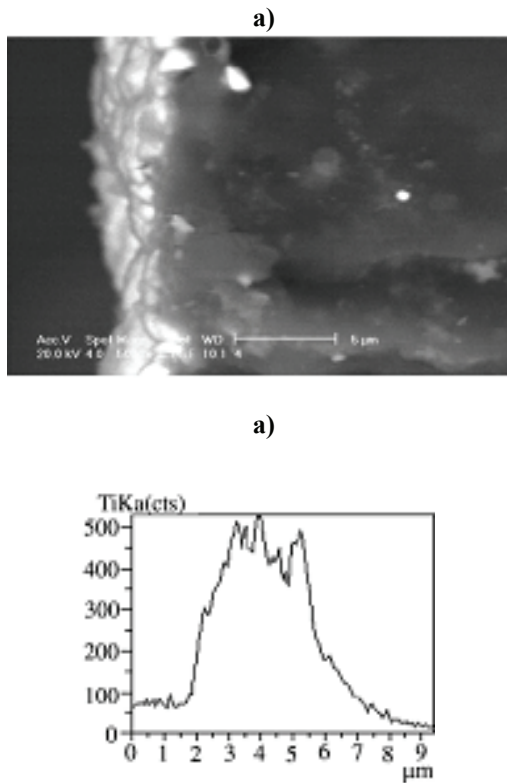
a)

a)

Fig. 4. SEM micrographs of the cross-section of the broken polyurethane samples with the TiN layer deposited by means of a Nd:YAG laser, with the thickness of 1μm (a) and the EDX line scan analysis through the thickness (b) (Major et al., 2004a)
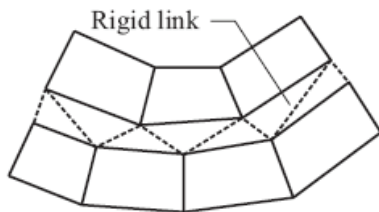

Fig. 5. Rigid link transfers stresses and connects layers (Bathe, 2004)

Each interlayer includes labelled layer. Physical properties of such layers are unknown. They are simulated as interlayer without properties in (Kopernik and Pietrzyk, 2006), like a contact space between main layers (Fig. 5.). Interlayer is shown as a free space, which connects two layers. It is made by rigid link algorithm in the programme. Rigid links are special constraint equations established automatically two nodes – a master node and a slave node. As the nodes displace due to deformation, the slave node is constrained to translate and rotate such that the distance between the master node and the slave node remains constant, and that the rotations at the slave node are the same as the corresponding rotations at the master node. Rigid links can be ki-

nematically linear or nonlinear (Bathe, 2004). For linear rigid links, the constraint equations are unchanged throughout the solution and hence they are applicable for small displacement analysis. In a large displacement analysis, nonlinear rigid links should be used recognizing that the effects of large displacements are taken into consideration in updating the constraint equations for the master and slave nodes.
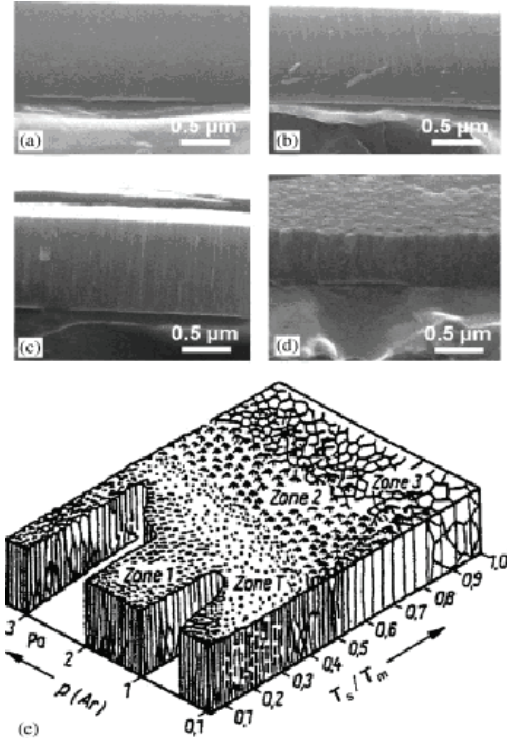

Fig. 6. Scanning electron microscopy (SEM) cross-section images of (a) Ti, (b) TiO$_2$, (c) on-axis deposited TiN (target and substrate surfaces parallel) and (d) off-axis deposited TiN (surfaces perpendicular). For comparison of the coating structures, the structure zone model developed by Thornton is shown in (e) (Lackner et al., 2004c), (Lackner, 2005c)

Experiments prove that interlayers are firm and provide compact connection. Even torsional deflection does not tear such material. Interlayer penetrates into main layer and that is why its thickness is decreased in simulation. Pseudodiffusion layer (additional interlayer's name) is a part of main layer (Major et al., 2004a). Sometimes (Cai and Bangert, 1996) interlayer properties are assumed to be the mean of the coating and substrate. Such approximation was also made in (Kopernik and Pietrzyk, 2006) for thin film of TiN/Ti.

FEM is used by (Paszyński et al., 2006) to predict behavior of TiN/Ti/PU. Nanomaterial works under static loading (left ventricle maximum pressure) (Fig. 7.). Dimensions of the sample used in the FEM analysis are presented in (Major and Lacki, 2005). During the analysis hp adaptive code de-

scribed in (Paszyński et al., 2006) and commercial code ADINA were used to evaluate differences between optimal meshes, which have been obtained for this problem. The computational mesh used in ADINA contains 49529 degrees of freedom. The same analysis has been performed based on the hp adaptive code (Paszyński and Demkowicz, 2006; Paszyński et al., 2006). The solution over the initial mesh shows almost no deformation of the top of the sample. Significant improvement in the quality of the results is observed after three iterations of the fully automatic hp adaptivity, the top of the body is deformed. There is a difference between ADINA and hp adaptive code results in maximum value of the displacement. The error estimations performed by the hp adaptive code show that there is 23% relative error in energy norm at the initial mesh, and after three iterations the error decreases to the level of 5%. The size of the final coarse mesh is 2918 degrees of freedom.
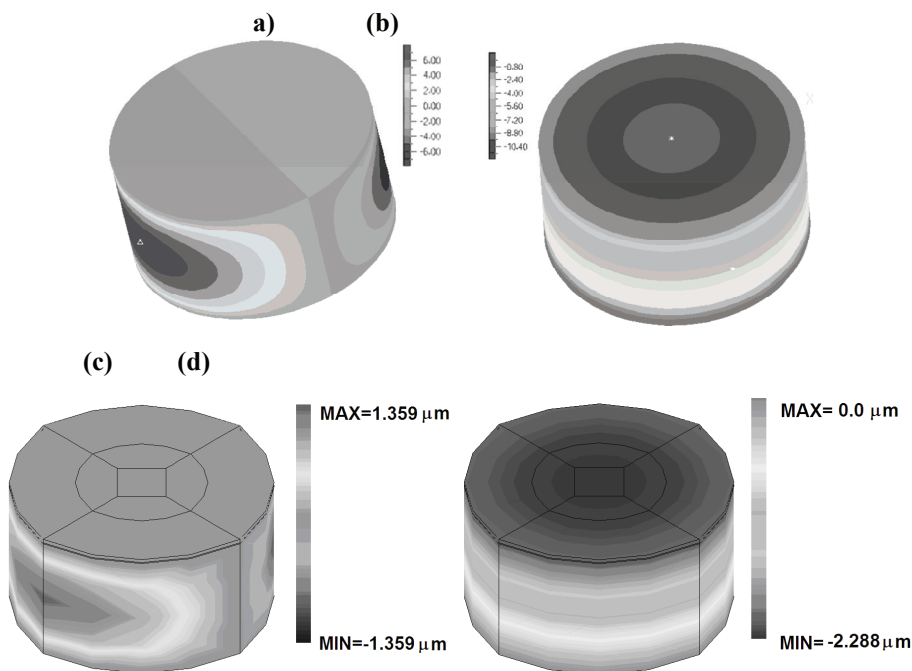
et al., (2001), because of the author's domain of study) deposited on soft substrates using:
− PVD (physical vapour deposition) (Zoesterbergen, 2000)
− CVD (chemical vapour deposition) (Santhanam et al., 1996), (Fang et al., 2004)
− PLD (pulsed laser deposition) (Major and Lacki, 2005)

are:
− mechanical properties (adhesion, hardness, residual stress, modulus of elasticity, etc.)
− physical properties (density, thermal expansion coefficient, melting point, friction coefficient, etc.)
− abrasive wear resistance (tribological properties)
− anticorrosive, diffusive, thermal protection
− structure, chemical constitution, thickness of layer.

Mechanical properties (hardness, stiffness, fracture resistance, toughness, load support) and tribological properties (friction coefficient, adhesion, resistance to: abrasive wear, sliding wear, brittle fracture, fatigue wear, dynamic loading and corrosion of thin film/coating systems) are obtained in the following test:
− nanoindentation
− nano-scratch
− nano-impact
− high temperature testing.

4.1. Nanoindentation test

Experimental methods related to nanoindenation test are desrcibed below, but not very precisely, because of other purpose, which is defined as indicating the most important problems in this thematic area. Interesting is an experimental-numerical approach to subject, as well as the numerical solutions.

Fig. 7. ADINA results: (a) Maximum X-displacement [μm], (b) Maximum Z-displacement [μm]; hp adaptivity results: (c) Maximum X-displacement [μm], (d) Maximum Z-displacement [μm] (Paszyński et al., 2006)

4.   NANOMATERIALS TESTS

With principles of knowledge related to FGM, especially graded thin films and modelling, there is a possibility to go to further analysis, which is desribing experimenatal and numercial techniques in nanomaterials research. Properties of hard coatings (Dobrzański, 2002) (for the most part TiN - Pollini

4.1.1. Experimental studies

The International Organization for Standardization (ISO) has produced an international standard ISO 14577 (Overview of Mechanical Testing Stan-

dards, 2002), (ISO/FDIS 14577-1:2002), which can be applied to instrumented indentation testing. The determination of properties is divided into three ranges:

− Macro range: 2 N < F < 30 kN,
− Micro range: 2 N > F; h > 200 nm,
− Nano range: h < 200 nm.

The indentation test can be controlled either in force or in depth. Experimental nanoindentation test gives the following parameters:

− mechanical properties (hardness, elastic modulus),
− creep resistance,
− temperature-dependent properties.

No other technique provides information about both the elastic and plastic properties of thin films.

The fourth most commonly used pyramidal indenter geometries are (Overview of Mechanical Testing Standards, 2002) such as Vickers, Berkovich, modified Berkovich and cube corner (Ning, et al., 2004). The Martens hardness is defined for Vickers and Berkovich indenter geometries but not for spherical or Knoop indenters.

Nanoindentation testing is performed in load-controlled mode using a NanoTest system (Beake and Lau, 2005). Indentations are 20-cycle load-controlled load-partial unload experiments from 1 mN to 20 mN maximum load. An uncoated substrate wafer is tested for comparison. The data are analysed with the Oliver and Pharr method (Oliver and Pharr, 1992) and repeat load-partial unload experiments are performed on each sample. The Oliver-Pharr method is widely used in depth sensing indentation machines with Berkovich indenter (Franco et al., 2004). Berkovich is deformable, elastic diamond, tip radius assume to 100-150 nm, effective cone angle is 140.64° (Fischer-Cripps, 2002). However, it is equally applicable to the case depth sensing indentation using a Vickers indenter, with good results. The depth sensing indentation machine used in this work analyses indentation data using a software based on the Doerner-Nix method (1986), and uses an incorrect area function to describe the indenter tip shape, leading to overestimated elastic modulus and hardness values due to ISE effect - indentation size effect (Iost and Bigot, 1996).

The work (Franco et al., 2004) aims to develop a computational routine based on the Oliver-Pharr method for measuring more precise values of elastic modulus and to obtain Vickers hardness numbers, using a depth sensing indentation apparatus, equipped with a Vickers diamond indenter.

In (Attaf, 2004b) an experimental method is being investigated for the tip geometry determination from depth sensing indentation data. To show the reasons of the existing geometry, an expression is proposed for Berkovich indenter volume and compared to the equivalent Vickers volume. An existing proportionality is emphasizing between the displaced volume of material and various values of the energy. The actual tip bluntness is then deduced by energy extrapolation and use is made of the energy amount proper to the apex missing part to introduce an appropriate correction to the indentation cycle model proposed. The aim of this correction is to adapt the model to a geometrically perfect indenter without tip truncation for more accuracy in nanomechanical properties calculation.

Another article (Attaf, 2004a) continues shallow indentatation process, but concentrate on simulating the load-displacement response of materials under indentation. Many formulas have been used: Kick's law, Bernhardt formula, Bűckle's empirical equation, Meyer's power law and their modified or corrected forms. It is shown that all these formulas are nothing but various truncated forms of an integer power series of the load in terms of penetration depth. This infinite series is an expansion of Meyer's power law which appears to be the most accurate relation for modeling the load-displacement curve. This peculiarity emphasizes the significance of the β-material concept in analyzing the materials behavior and allows a better understanding of the hardness value change with the loading curve model.

As well as above relations among variables reached in nanoindenatation test other investigations are being made (Bao et al., 2004). An analytical relationship between the reduced modulus E_r and hardness H for solid materials is established based on the conventional depth-sensing indentation method of Oliver and Pharr. It is found that the two properties are related through a material parameter that is defined as the recovery resistance R_s. This parameter represents the energy dissipation during indentation. A simple set of procedures to determine the area of indent is also presented. The procedures require three measured quantities, i.e., the peak load, corresponding displacements and the depth of residual indentation. Complicated curve fitting and regression analysis, which themselves involve the specimen material, is not required. Nanoindentation tests were performed using a Berkovich indenter on five materials spanning a wide range of hardness and plasticity. Experimental results revealed two impor-

tant features: (a) the reduced modulus predicted by the new E_r-H relationship is the same as that obtained by the conventional method; (b) the elastic modulus and hardness values determined by the simple set of procedures are comparable to those obtained by using the conventional method.

4.1.2. Numerical studies

The nanoindentation process of a soft coating on a harder substrate has been simulated by the finite element method (Panich and Sun, 2004). The frequently used three-face Berkovich indenter was simulated by an axisymmetric conical indenter with the same projected area depth function. The paper discusses the critical indentation depth below which the substrate has negligible effect on the indentation response of layered systems. The influence of the yield strength ratio of the soft coating to the harder substrate and the indenter tip radius in the critical depth were analysed. Two distinctly different relationships between the critical depth and the yield strength ratio of the coating to the substrate were noted. Analysis reveals that these two different regimes are derived from the two dominant substrate effects on indentation response, i.e. the initiation and propagation of plastic deformation in the substrate, and the enhanced material pile-up around the indenter.

Frictional effects on sharp indentation of strain hardening solids are examined in (Mata and Alcalá, 2004). The results of finite element simulations in a wide range of solids allow to derive two equations accounting for the influence of the friction coefficient on the determined hardness. Comparisons between the simulations and micro-indentation experiments are undertaken to ensure the validity of the former to metallic materials.

An accurate representation of the indenter shape (Ning et al., 2004) is essential for correct finite element simulations of shallow indentations of less than 50 nm using a 90° cube-corner indenter. A nonlinear regression method for estimating the tip radius of an indenter is presented in (Ning et al., 2004), which takes into account that initially the contact is only with the spherical surface of the tip and subsequently also includes contact with the equivalent conical surface. The tip radius of a Berkovich indenter is estimated by a finite element modeling (FEM) best-fitting method. Using the estimates of tip radii, the yield strength of gold in the film of a gold/silicon system was estimated from the best fit between FEM simulations and nanoindentation ex-

periments using the 90° cube corner indenter, which compared well with an FEM simulation and nanoindentation data using a Berkovich indenter.

The finite element method for elasto-plastic large strain was employed to study the indentation experiment of Al film on Si substrate by a rigid spherical indenter (Ma et al., 1998). The relationships between mechanical properties of the film and the values of the load-displacement curve have been obtained. The hardening index and yield strength of the metal film are determined.

The advanced computational study is shown by (Dao et al., 2001). It is undertaken to identify the extent to which elasto-plastic properties of ductile materials could be determined from instrumented sharp indentation and to quantify the sensitivity of such extracted properties to variations in the measured indentation data. Large deformation finite element computations are carried out for different combinations of elasto-plastic properties that encompass the wide range of parameters commonly found in pure and alloyed engineering metals: Young's modulus, yield strength, strain hardening exponent and the Poisson's ratio. Using dimensional analysis, a new set of dimensionless functions and elasto-plastic finite element computations, analytical expressions were derived to relate indentation data to elasto-plastic properties. Forward and inverse analysis algorithms were thus established; the forward algorithms allow for the calculation of a unique indentation response for a given set of elasto-plastic properties, whereas the inverse algorithms enable the extraction of elasto-plastic properties from a given set of indentation data. A representative plastic strain was identified as a strain level, which allows for the construction of a dimensionless description of indentation loading response, independent of strain hardening exponent. The proposed inverse analysis provides a unique solution of the reduced Young's modulus, the representative stress and the hardness. These values are somewhat sensitive to the experimental scatter and/or error commonly seen in instrumented indentation. With this information the assumption of power law hardening adequately represents the full uniaxial stress-strain response. These plastic properties, however, are very strongly influenced by even small variations in the parameters extracted from instrumented indentation experiments. Comprehensive sensitivity analyses are carried out for both forward and inverse algorithms, and the computational results are compared with experimental data for two materials.

The deformation underneath a spherical indent was investigated on samples prepared by the bonded-interface technique from a plasma sprayed nickel-5% aluminum coating (Prchlik et al., 2003). Prior to the spherical indentation a set of Vickers micro-indents was produced as fiduciaries on one of the cross-sections. This allowed the calculation of plastic strain components from the relative displacements of micro-indents during subsequent surface indentation. Using a modified procedure based on a method proposed by Tabor (1951) stress-strain curve was evaluated by measuring the contact radii of spherical indentations produced at several different loads. The derived stress-strain relationship was used in 2D and 3D finite element models to estimate the plastic deformation field under the indenter. The comparison between the measured and calculated strain profiles revealed notable differences. The normal plastic strain in the direction along the vertical axis of indentation displayed higher values directly under the indenter compared to the finite element analysis which predicted lower values under the indenter and less rapid decrease of the plastic strain with depth. The differences were attributed to the compaction of the lamellar structure in the plasma sprayed coatings. The compaction of the lamellae was directly observed on polished coating cross-sections. The finite element technique gives results compared to experimental data.

4.1.3. Experimenatal and numercial studies

Many authors deal nanoidenatation as double subject: experiment and modeling. Shallow finite element analysis is taken in (Lichinchi et al., 1998), (Fazio et al., 2001) and (Gong et al., 2004). In fact an experimental nanoindetation is a multistages' process, the indenter penetrates deeply into investigated material and additionally the specimen is a complex structure. Mentioned test's conditions go to conclusion that such experiment is not easy to be simulated by convencional, numerical methods, especially deep penetration causes numerical problems. Performed and presented in articles, numerical experiments should be named shallow finite element analysis, because they have limitations, which are shown for example, when load-displacement curves are presented. Most authors have only first stage - first indetation step and such curve can be obtained by convencional FEM methods. Some of them present more results, but they just arises from repetition of the first step. Exactly experimental nanoindetation

test is deep nanoindetation and numerical one is shallow nanoindentation. Both methods can be correctly compared only in first nanoindentation step.

In (Lichinchi et al., 1998) the comparsion between the experimental data and numerical results for TiN/HSS demonstrated that the finite element approach is capable of reproducing the loading-unloading behavior of a nanoindentation test.

Fazio et al. (2001) described an experimental procedure for the determination of the hardness and the elastic modulus through nanoindentation of a CVD diamond coating using simple analytical formulae. Such tests, performed with a Berkovich indenter, were simulated by finite element analysis. Through the numerical analysis, it was possible to reproduce the load-penetration depth curves and, thus confirm the validity or correct the property calculations. Results show that the predicted property values can be affected by the assumed material strain hardening. By comparing the numerical values with the experimental results, it is possible to characterize, with sufficient accuracy, the material behavior.

Nanoindentation data measured on soda-lime glass were analyzed by Gong et al. (2004) by assuming that the test material has a load-independent hardness number. The area function was established with a simple analysis method. It was shown that the deviations of the determined area function from the perfect Berkovich geometry may be attributed to two factors: the indenter tip rounding and the deformation of the indenter during indentation.

4.1.4. Nanoindetation for multilayer system

Multilayer systems are also being simulated and investigated (Vieira and Ramos, 1999), (Bull et al., 2004), (Martinez et al., 2003). Such materials are demanding in experiments and simulations, but have the most interesting characteristics and applications.

Multilayers between ceramic materials and metallic materials (Vieira and Ramos, 1999) can combine the high hardness and wear resistance of the ceramic layers with the toughness and mechanical strength of the metallic layers. This work is aimed at the production and characterization of tungsten nitride/titanium (or nickel) multilayers. The coatings, deposited by magnetron sputtering, are characterized with respect to their structure, morphology and hardness. The adhesion to the substrate is evaluated by a scratch-test technique, as it constitutes a fundamental prerequisite. The choice of titanium and

nickel as interlayering materials was made in order to study the role of materials with elevated plasticity, but with different reactivities. Titanium tends to react chemically with other materials, namely, ferrous oxides and nitrides. Nickel has low chemical reactivity but has the same crystallographic structure as the W_2N phase. All of the multilayer coatings produced have a total thickness of 4μm. The hardness of the multilayers, deposited with different ceramic/metal thickness ratios, decreases with the thickness of the ductile metallic layers. When the metal thickness is too high it causes the spalling of the coatings. The optimal medium critical load (65 N) is obtained with a ceramic/metal ratio equal to four. Even though the type of bond is different, the adhesion of the multilayers is not influenced by the substitution of titanium with nickel. The deposition process yields well-adhered and sufficiently hard multilayer coatings when compared with the ceramic single layers.

Many coatings and surface treatments have been developed to enhance component performance and, increasingly, coating architectures are becoming more complex as multilayer, superlattice and graded coating systems become widely available. There are so many potential coating variants that it is almost impossible to test all the possibilities to optimize performance. Therefore the need for predictive performance models is increasing but model development has generally lagged behind the introduction of new coatings. For tribological coatings, the mechanical response to contact is particularly important if performance has to be understood. Bull et al. (2004) briefly reviews developments in numerical simulation and extends recent modeling developments in an energy-based predictive model for the hardness and Young's modulus of a coated system. The model can be applied to a single layer of multilayer coatings successfully. Model predictions can be improved by considering the through-thickness fracture behavior of the coating.

The mechanical behavior of CrN/Cr multilayer coatings deposited by magnetron sputtering has been investigated by nanoindentation measurements performed with indenters of different geometries (Martinez et al., 2003). Nanoindentation stress-strain curves generated from these measurements allow to characterize the complete mechanical behavior of these coatings in the elastic, elasto-plastic, plastic and fracture deformation regimes. Indentation measurements carried out with a spherical indenter allowed to study the elastic deformation regime and

estimate the yield stress parameter through the initial indentation yielding point. The elasto-plastic deformation regime was studied using a spherical indenter and the stationary yielding regime (fully plastic regime) was investigated with a pyramidal indenter of Berkovich geometry. The use of a pyramidal cube-corner indenter allowed to study coating fracture characteristics. Nanometric CrN/Cr multilayer structures as well as single CrN and Cr coatings have been characterized. The study showed that multilayered coatings with period thickness less than 46nm present values of yield stress, Young's modulus, hardness and toughness higher than those for single-layer CrN and Cr coatings.

4.2. Nano-scratch test – compatibilty between experiment and simulation

In experiment, the diamond probe is scanned across the surface under either a constant load or a progressively increasing load until film failure occurs. Scratching at different locations at constant load can be used to investigate coating quality and homogeneity. By ramping the load it is possible to define a critical load for adhesive failure of the coating-substrate system. Failure can be detected by: (a) by the detection of an abrupt change in the displacement of the probe; (b) by a sudden change in the frictional force between the diamond and the surface; (c) by microscopic observation of the wear track; or (d) by detection of a burst of released acoustic energy.

In the scratch tester contact of a diamond spherical tip moving with increased load on a titanium nitride (TiN) coated steel surface is investigated (Holmberg, 2000; Holmberg et al., 2003). The model considers elastic, plastic and fracture behavior of the contacted surface. The stress field in the coated surface is formed as a result of the following four effects:

1) The friction between the sliding tip and the surface results in compression stresses from the pushing force in front of the tip and tension stresses from the pulling force behind the tip.

2) The elastic and plastic deformations are spherical indent, groove and torus shaped. The stresses are both compressional and tensional.

3) The spherical indentation pattern causes the substrate to deform plastically, reaching its peak value at an angle of about 45° from the plane of symmetry in the plane of the coating.

4) It is very common especially for thin ceramic coatings that they, due to the deposition process,

contain even very considerable compressional residual stresses. These are typically of the order of 0.5-3 GPa, but values even as high as 10 GPa may appear (Holmberg, 2000; Holmberg et al., 2003).

The computer simulations of the stresses and strains in the surface illustrate well what kind of load situations and deformations a surface is exposed to when a spherical counter surface is sliding over it. The stress fields result in elastic and plastic deformations that change the shape of the surface. The stresses in addition to the state of deformation are the origin to possible crack generation and crack propagation in the coating, at the coating/substrate interface or in the substrate. When cracks grow due to increased stresses and unite with other cracks, debris is formed and they may detach from surface. This is the origin of the process wear.

TiB$_2$-based nanostructure coatings were fabricated on high-speed steel magnetron sputtering technique (Panich and Sun, 2006). Mechanical characterization of the resultant coating-substrate systems (coating adhesion, friction, scratch resistance) is conducted by microscratch technique. The linearly increasing load mode of microscratch test is studied to determine testing conditions and the critical load for coating failure. The mode of failure is examined by high resolution SEM and AFM. The three-dimensional FE model is developed to simulate the scratch process and is able to demonstrate the elastic and plastic behavior of the coating and substrate around the contact area during scratch test. Good agreement between the FEA and experimental investigations is observed.

4.3. Nano-impact test - experiment

Thin films and coatings can fail by fatigue at lower loads than predicted by static tests (Beake and Smith, 2004). The nano-impact technique is a low load impact test capable of revealing marked differences in performance that can be used to optimize the design of coating systems for improved durability. Instead of simply "characterizing" coatings and thin films, their actual tribological performance under "in-service" conditions can be assessed. The technique can be used to find the optimum coating process parameters for enhanced toughness and damage tolerance and can also differentiate between cohesive (chipping) and adhesive failure (delamination). The concepts behind the nano-impact technique are introduced and results are presented on

compositionally graded coatings on tool steel. The performance of the CrAlTiN system was dependent on the impact load.

The a-C showed greatly improved impact resistance compared to the a-C:H coating due to its graphite-like structure. A repetitive contact technique has been used to investigate the fracture properties of tetrahedral amorphous carbon (ta-C) thin films deposited on silicon by the filtered cathodic vacuum arc method (Beake et al., 2004). The impact test is showing differences in the resistance to impact wear of ta-C films with their thickness. The resistance to impact-induced fracture decreases as the film thickness increases. This may be due to the maximum shear stress being closer to the film-substrate interface, or reflect reduced toughness in the thicker films that are less able to deform as the substrate deforms plastically during the repetitive contact test. The mechanism of impact-induced failure on such thin films is (a) the initial impact stage where plastic deformation causes cracks to nucleate sub-surface, (b) fatigue-further nucleation and growth of sub-surface cracks (with little or no change in probe depth) and (c) crack coalescence and film fracture leading to a change in probe depth as the film fails. Fracture probability increases sharply as the impact load is increased from 100 to 300 mN. The greater load provides the stresses to nucleate and propagate the sub-surface cracks; at low load the driving force for the cracks to coalesce and spall the coating is much reduced, so failure is less likely to occur within the test duration.

4.4. Direct problem and final objective

Experimental nanoindetation is a multistage process, indenter penetrates deeply into testing material and specimen is a multilayer structure. Very thin adjacent layers and conditions of the test allow statement that this experiment is not easy to be simulated by finite element method. Therefore, authors reduce numerical analysis to shallow nanoindentation test and do not reconstruct experiment in complete range. After such operation obtained data numerical are related only to the first nanoindenation stage. Having these results, further analysis include computing mechanical properties of investigated materials, but the consequent results are not very interesting, because of the numerical character of the test. Carrying only shallow nanoindetation the output information is not complete and important reactions of bottom layers are missed, which are very

meaningful, because of the properties – elasto-plastic, or mixed layers elastic and elasto-plastic. Many of those researchers even do not show very deformed meshes, they give only demostrative pictures and graps, without publishing the most interesting details (like mentioned above). In fact most of authors have only first stage - first indentation step and such single curve can be obtained by convencional FEM methods. Some of them present more results, but they just arises from repetition of the first step. Concluding, experimental nanoindetation test is a deep nanoindetation and the numerical one is a shallow nanoindentation. Both methods can be correctly compared only in the first step.

The authors of this paper make an affort to get full range of nanoindentation test numerically. The model is now being developed, improved and modified (Fig. 8.). This is an initial stage to get the complete model, which can be compared to experimental deep nanoindetation test. Some simplifications were done, like 2D, reduction of the layers number, simplified indenter shape, and character of the results is an effect of these simplifications. Deformed mesh from previous computing step is set as an initial mesh to the next computing step, as well as stresses, and such procedure is repeated as many times as is required in an experiment. Number of stages is releated to material character and is not a constant number. Some other problems have to be solved and finally correct, full load-displacement curve for multistage numerical simulation of nanoindentation test will be obtained.

The final objective of the work goes further – to prepare models for the inverse analysis. Authors intention is to get the mechanical properties of graded nanomaterials in deep nanoindentation numerical test. Mechanical properties of each material in multilayer system are not well known, and they have to be calulated having only the character of experimental results obtained in nanoindentation test. The numerical finite element model in deep nanoindetation test needs precise input material properties and correct material models. The inverse analysis (Szeliga and Pietrzyk, 2002) will be helpful in achieving these informations. At the beginning the problem can be defined as:

− searching for values of system parameters for known input and output data (problem of identification of object parameters)
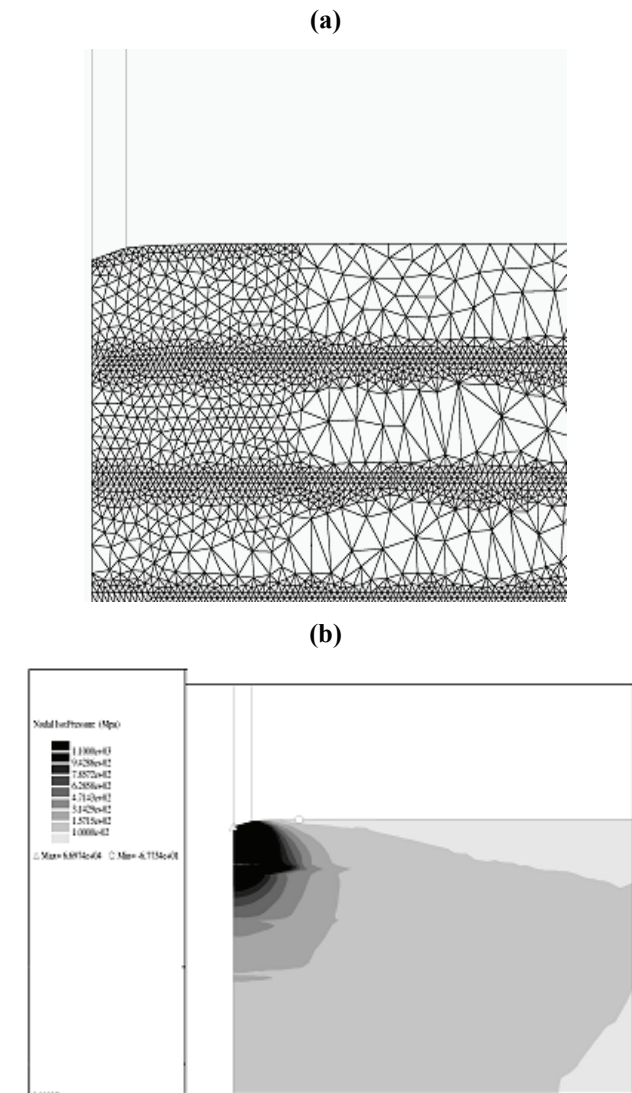
or as:

(a)

(b)

Fig. 8. Cutting (6 layers) of 2D, axisymmetric, numerical model of multilayer system (11 layers), a) Specimen deformed mesh after 20 indents and outline of moving, deformable die (die mesh in not visible) are shown, b) Distribution of pressure (average stress), after unloading in specimen is calculated. Maximum values of computed quantity are concentrated in thin layers, these elasto-plastic ones. Elastic layers only transmit loadings.

− calculation of values of input data based on output data and known system factors (reconstruction problem)

and this task is named inverse problem. The algorithm, which solves the problem, is called inverse method. Practically this task will be working out in such steps:

− set available input material parameters into numercial model, which is constructed possibly precisely and corresponds with the experimental one,

− when output numerical data agree with the experimental results, set those values into inverse algorithm and find system factors,

− change input parameters according to estimated rheological factors of constitutive equation,

− repeat these steps until the output data are close to experimental results.

After this procedure is made, the final objective is reached.

5. CONCLUSIONS

After making the review of research on FGMs and performing FEM simulations, the direct problem is formulated and, partly, but correctly solved by the authors. The final aim of the work is obtained and will be realized by improving direct problem (finite element model) and finally using inverse method in further analysis. Presented results of simulations show that, after rescaling, the FEM program is capable to simulate properly deformation of materials in nano-scale. Load-displacement relationship is calculated and distribution of strains around the tool is determined.

The two ways of solutions, the direct problem described in this work and the optimization algorithm presented in (Szeliga and Pietrzyk, 2002), will be connected and the procedure will be integrated and automatized and the inverse tool for the nano-indentation tests will be developed.

ACKNOWLEDGEMENTS

LITERATURE

Argyris, J., Doltsinis, I.S., Eggers, M., Handel, R., 1994, *Computer Meth. Appl. Mech. Eng*., 111, 203.

Attaf, M.T., 2004a, Connection between the loading curve models in elastoplastic indentation, *Materials Letters*, 58, 3491–3498.

Attaf, M.T., 2004b, Tip bluntness determination using the energy principle and consequent correction to the indentation function, *Materials Letters*, 58, 1100–1106.

Bansal, Y. , Pindera, M.-J., 2003, Efficient formulation of the thermoelastic higher-order theory for functionally graded materials, *J. Thermal Stresses*, 26, 1055-1092.

Bao, Y.W., Wang, W., Zhou, Y.C., 2004, Investigation of the relationship between elastic modulus and hardness based on depth-sensing indentation measurements, *Acta Materialia*, 52, 5397–5404.

Basu, S.K., Scriven, L.E., Francis, L.F., McCormick, A.V., 2005, Mechanism of wrinkle formation in curing coatings, *Progress in Organic Coatings*, 53, 1-16.

Bathe, K. J., 2004, *Adina Theory and Modeling Guide*, Report ARD 04-7, 1.

Bathe, K.J., Montans, F.J., 2004, On modeling mixed hardening in computational plasticity, *Computers and Structures*, 82, 6, 535 – 539.

Beake, B.D., Lau, S.P., Smith, J.F., 2004, Evaluating the fracture properties and fatigue wear of tetrahedral amorphous carbon films on silicon by nano-impact testing, *Surface and Technology*, 177-178, 611-615.

Beake, B.D., Smith, J.F., 2004, Nano-impact testing – an effective tool for assessing the resistance of advanced wear-resistance coatings to fatigue failure and delamination, *Surface and Coatings Technology*, 188-189, 594-598.

Beake, B.D., Lau, S.P., 2005, Nanotribological and nanomechanical properties of 5–80nm tetrahedral amorphous carbon films on silicon, *Diamond and Related Materials*, 14, 1535–1542.

Bull, S.J., Berasetegui, E.G., Page, T.F., 2004, Modeling of the indentation response of coatings and surface treatments, *Wear*, 256, 857–866.

Butcher, R.J., Rousseau, C.E., Tipper, H.V., 1999, A functionally graded particulate composite: preparation, measurement and failure analysis, *Acta Materialia*, 47, 259-268**.**

Cai, X., Bangert, H., 1996, Finite-element analysis of the interface influence on hardness measurements films, *Surface and Coatings*, 81, 240-255.

Carneiro, C.A.V., Rochinha, F.A., Borges, L.S.A., 2004, Thermoelastic analysis of functionally graded materials submitted to shocks, *Proc. 21st ICTAM, SM10 Functionally Graded Material*s, 1-2.

Cheng, Z.-Q., Batra, R.C., 2000, Three-dimensional thermoelastic deformations of a functionally graded elliptic plate, *Composites: Part B*, 31, 97-106.

Czarnowska, E., Wierzchoń, T., Maranda-Niedbała, A., 1999, Properties of the surface layers on titanium alloy and their biocompatibility in vitro tests, *J. Mat. Proc. Techn*., 92-93, 190-194.

Dao, M., Gu, P., Maewal, A., Asaro, R.J., 1997, A micromechanical study of residual stresses in functionally graded materials, *Acta Materialia*, 45, 3265-3276.

Dao, M., Chollacoop, N., van Vliet, K.J., Venkatesh, T.A., Suresh, S., 2001, Computational modeling of the forward and reverse problems in instrumented sharp indentation, *Acta Materialia*, 49, 3899–3918.

Delale, F., Erdogan, F., 1983, The crack problem for nonhomogeneous plane, *J. Appl. Mech.*, 50, 609-614.

Dobrzański, L.A., 2002, *Podstawy nauki o materiałach i metaloznawstwo*, Podręcznik akademicki, Gliwice-Warszawa (in Polish).

Doerner, M. F., Nix, W. D., 1986, A method for interpreting the data from depth-sensing indentation instruments, *J. Mater. Res.,* 1/4, 601-609.

Drysdale, W.H., Zak, A.R., 1985, Structural Theories - A Theory for Rate Dependent Plasticity, *Computers and Structures*, 20, 259-264.

Eischen, J.W., 1987, Fracture of nonhomogeneous materials, *Int. J. of Fracture*, 34, 3-22.

Erdogan, F., 1995, Fracture mechanics of functionally graded materials, *Composite Eng.*, 5, 753-770.

Erdogan, F., Wu, B.H., 1997, The surface crack problem for plate with functionally graded properties, *J. Appl. Mech*., 64, 449-456.

Fang, T.H., Jian, S.-R., Chuu, D.-S., 2004, Nanomechanical properties of TiC, TiN and TiCN thinfilms using scanning probe microscopy and nanoidentation, *Appl. Surface Science*, 228, 365-372.

De Fazio, L., Syngellakis, S., Wood, R.J.K., Fugiuele, F.M., Sciumé, G., 2001, Nanoindentation of CVD diamond: comparison of an FE model with analytical and experi-

mental data, *Diamond and Related Materials*, 10, 765-769.

Fischer-Cripps, A.J., 2002, *Nanoindentation*, Springer-Verlag, ISBN 0-387-95394-9.

The FORGE® V.2.4 materials database, 2004, Tranvalor SA of Sophia-Antipolis, France.

The FORGE® V.3.6 materials database, 2005, Tranvalor SA of Sophia-Antipolis, France.

http://www.matweb.com.

Franco, A.R., Pintaúde, G., Sinatora, A., Pinedo, C.E., Tschiptschin, A.P., 2004, The Use of a Vickers Indenter in Depth Sensing Indentation for Measuring Elastic Modulus and Vickers Hardness, *Materials Research*, 7, 483-491.

Gdoutos, E.E., Daniel, I.M., Wang, K.-A., 2003, Compression facing wrinkling of composite sandwich structures, *Mechanics of Materials*, 35, 511-522.

Gere, J.M., Timoshenko, S.P., 1984, *Mechanics of Materials*, PWS-KENT Publishing Company, Boston.

Ghista, D.N., Reul, H., 1983, Prosthetic aortic leaflet valve design: performance analysis of an Avcothane® leaflet valve, *Adv. Cardiovasc. Phys*., 5 (IV), 31-42.

Gong, J., Miao, H., Peng, Z., 2004, On the contact area for nanoindentation tests with Berkovich indenter: case study on soda-lime glass, *Materials Letters*, 58, 1349–1353.

Gu, Y.Y., Lin, J.F., 1996a, The tribological characteristics of titanium nitride coatings, *Wear*, 194, 22-29.

Gu, Y.Y., Lin, J.F., 1996b, Comparsion of the tribological characteristics of titanium nitride and titanium carbonitride coating films, *Surface and Coating Techn*., 85, 146-155.

Gu, Y.Y., Lin, J.F., Ai, C.-F., 1996, The tribological characterisctics of titanium nitride coatings, *Wear*, 194, 12-21.

Gu, P., Asaro, R.J., 1997, Cracks in functionally graded materials, *Int. J. Solids and Structures*, 34, 1-7.

Gu, P., Dao, M., 1999, A simplified method of calculating the crack tip field of functionally graded materials using domain integral, *J. Appl. Mech*., 66, 101-108.

Hansel, A., Spittel, T., 1978, *Krafts und Arbeitsbedarf Bildsamer Formgebungsverfahren VEB Deutscher Verlay fűr Grundstoff Industrie*, Leipzig.

Hirano, T., Yamada, T., Teraki, J., Mino, M., Kumakawa, A., 1988, *Proc. 16th Int. Symp. on Space Technology and Science*, Tokyo, 375-380.

Ho, S.P., Balooch, M., Marshall, S. J., Marshall, G.W., 2004, *Local properties of a functionally graded interphase between cementum and dentin*, Wiley InterScience 1**,** www.interscience.wiley.com

Holmberg, K., Matthews, A., 1994, Coatings tribology properties, techniques and applications in surface engineering, *Elsevier Tribology Series 28*, *Elsevier Science B.V.*, The Netherlands, 442.

Holmberg, K., Matthews, A., Ronkainen, H., 1998, Coatings tribology-contact mechanisms and surface design, *Tribology Int*., 31, 107–120.

Holmberg, K., 2000, The basic material parameters that control friction and wear of coated surfaces under sliding, *Tribologia-Finnish*, *J. of Tribology*, 19, 3-18.

Holmberg, K., Ronkainen, H., Matthews, A., 2000, Review Tribology of thin coatings, *Ceramics Int*., 26, 787-795.

Holmberg, K., Laukkanen, A., Ronkainen, H., Wallin, K., Varjus, S., 2003, A model for stresses, crack generation and fracture toughness calculation in scratched TiN coated steel surfaces, *Wear*, 254, 278-291.

http://cardiotech-inc.com/products/chronothanep.asp

http://www.ptli.com:

http://www.ptli.com/testlopedia/tests/DurometerShore-d2240.asp

http://www.ptli.com/testlopedia/tests/tensile-rubber-D412.asp

http://www.ides.com/plasticsweb/property_help/ASTMD624.htm

http://www.ides.com/plasticsweb/property_help/ASTMD1525.ht

mhttp://www.ptli.com/testlopedia/tests/Flex-D790.asp

Inagaki, M., Yokogawa, Y., Kameyama, T., 2003, Formation of highly oriented hydroxyapatite in hydroxyapatite/titanium composite coating by radio-frequency thermal plasma spraying, *Journal of Materials Science: Materials in Medicine*, 14, 919-922.

Iost, A., Bigot, R., 1996, Indentation size effect: Reality or artefact?, *J. Mat. Sci*., 31, 3573-3577.

ISO/FDIS 14577-1:2002; *Metallic materials - Instrumented indentation test for hardness and materials parameters*, ISO Central Secretariat, Rue de Varembé 1, 1211 Geneva.

Jin, Z.H., Batra, R.C., 1996, Some basic fracture mechanics concepts in functionally gradient materials, *J. Mech. Physics Solids*, 44, 1221-1235.

Kawasaki, A., Watanabe, R., 1997, Concept and P/M fabrication of functionally gradient materials, *Ceramics Int*., 23, 73-83.

Kesler, O., Matejicek, J., Sampach, S., Suresh, S., Gnaeupel-Herold, T., Brandt, P.C., Prask, H.J., 1998, Measurement of residual stress in plasma-sprayed metallic, ceramic and composite coating, *Mat. Sci. Eng*., A257, 215-224.

Kieback, B., Neubrand, A., Riedel, H., 2003, Processing techniques for functionally graded materials, *Mat. Sci. Eng*., A362, 81-105.

Kirchoff, G., Göbel, T., Bahr, H.A., Balke, H., Wetzig, K., Bartsch, K., 2004, Damage analysis of thermally cycled (Ti,Al)N coatings-estimation of strength and interface fracture toughness, *Surface Coat. Techn*., 179, 39-46.

Kobel'skij, S.B., Kuriat, R.I., Kravchenko, B.I., Kvitka, A.L., 1999, Procedure and analysis of three dimensional thermal stressed states of turbine blades with coatings subjected to thermal cycling, *Strength of Materials*, 31/6, 564-570.

Kohr, K.A., Gu, Y.W., 2000, Effect of residual stress perfomance of plasma sprayed functionally graded ZrO_2/NiCoCrAlY coating, *Mat. Sci. Tech*., A277, 64-76.

Kopernik, M., Pietrzyk, M., 2006, Możliwości modelowania nanomateriałów gradientowych, *Proc. 13th Conf. KomPlasTech*, ed., Szeliga, D., Pietrzyk, M., Kusiak, J., Szczawnica, 291-296 (in Polish).

Kravchuk, L.V., Buisikikh, K.P., Semenov, G.R., Borisov, Yu.S., Zadvornyi, A., 1999, Investigation of the thermal cyclic life of coatings for combustion chambers of gas turbines, *Strength of Materials*, 31/1, 43-48.

Kravchuk, L.V., Semenov, G.R., Borovkov, V.A., 994, Influence of heat-resistant coatings on the state of thermal stress of model of gas turbine engine blades in nonsteady heat exchange, *Strength of Materials*, 26/6, 418-423.

Kustosz, R., Major, R., Wierzchoń, T., Major, B., 2004, Designing a new heart, *Academia*, 3/3, 14-17.

Lackner, J.M., Waldhauser, W., Lenz, W., Ebner, R., Major, B., Schöberl, T., 2002, Deposition of TiN thin films on three dimensional shaped tools by pulsed laser deposition, *Oral Presentation at Materials Week 2002*, Munich (ICM), 378.

Lackner, J.M., Waldhauser, W., Berghauser, R., Ebner, R., Major, B., Schöberl, T., 2004a, Structural, mechanical and tribological investigations of pulsed laser deposited titanium nitride coatings, *Thin Solid Films*, 453 –454, 195–202.

COMPUTER METHODS IN MATERIALS SCIENCE

Lackner, J.M., Waldhauser, Ebner, R., Keckes, J., Schöberl, T., 2004b, Room temperature deposition of (Ti,Al)N and (Ti,Al)(C,N) coatings pulsed laser deposition for tribological applications, *Surface Coatings Techn.*, 177–178, 447–452.

Lackner, J.M., Waldhauser, W., Ebner, R., Major, B., Schöberl, 2004c, Structural, mechanical and tribological investigations of pulsed laser deposited titanium nitride coatings, *Surface and Coatings Techn.*, 180-181, 585.

Lackner, J.M., 2005a, *Industrially-scaled hybrid Pulsed Laser Deposition at room temperature*, Orekop, Kraków.

Lackner, J.M., 2005b, Influences of the nitrogen content on the morphological, chemical and optical properties of pulsed laser deposited silicon nitride thin films, *Surface and Coatings Technology,* 192*,* 225-230.

Lackner, J.M., 2005c, Industrially-styled room-temperature pulsed laser deposition of titanium-based coatings, *Vacuum*, 78, 73–82.

Landau, L.D., Lifshitz, E.M., 1986, *Theory of Elasticity*, Pergamon Press, Oxford.

Lee, W.Y., Stinton, D.P., Berndt, Ch.C., Erdogan, F., Lee, Y.D., Mutasim, Z., 1996, Concept of functionally graded materials for advanced thermal barrier coating appliacations, *J. Amer. Cer. Soc.*, 79, 3003-3012.

Li, J., Luo, X.Y., Kuang, Z.B., 2001, A nonlinear model for porcine aortic heart valves, *J. Biomechanics*, 34, 1279-1289.

Lichinchi, M., Lenardi, C., Haupt, J., Vitali, R., 1998, Simulation of Berkovich nanoindenattion experiments on thin films using finite element method, *Thin Solids Films*, 333, 278-286.

Ma, D., Xu, K., He, J., 1998, Numerical simulation for determining the mechanical properties of thin metal films using depth-sensing indentation technique, *Thin Solid Films*, 323, 183-187.

Markworth, A.J., Ramesh, K.S., Parks, W.P., 1995, Review Modeling studies applied to functionally graded materials, *J. Mater. Sci.*, 30, 2183-2193.

Major, B., Ebner, R., 1999, Laser applications in surface modification and pulsed laser deposition, *J. Technical Physics, Special Supplement XL. 3*, 161, Warszawa.

Major, B., 2002, *Ablacja i osadzanie laserem impulsowym*, Wydawnictwo Naukowe Akapit, Kraków (monograph in Polish).

Major, B., Bonarski, J.T., Waldhauser, W., Lackner, J. K., Ebner, R., 2004a, Contribution pulsed laser deposition conditions to texture, morphology and residual stresses developed in TiN thin layers, *Arch. Metall. Mater.*, 49, 83.

Major, B., Mroz, W., Wierzchoń, T., Waldhauser, W., Lackner, J. K., Ebner, R., 2004b, Pulsed laser deposition of advanced titanium nitride thin layers, *Surface Coatings Techn.* 180–181, 580–584.

Major, B., 2005, Laser technology in generating microstructure of FGM, *Arch. Metall. Mater.*, 50, 35-46.

Major, R., Kustosz, R., Major, B., 2003, Biozgodne cienkie warstwy wytwarzane na tytanie metalicznym i poliuretanie metodą osadzania laserem impulsowym, *Inżynieria Biomateriałów*, 30-33, 103-104 (in Polish).

Major, R., Lacki, P., 2005, Finite-element modeling of thin films deposited on the polyurethane substrate, *Arch. Metall. Mater.*, 50, 379-385.

Martinez, E., Romero, J., Lousa, A., Esteve, J., 2003, Nanoindentation stress–strain curves as a method for thin-film complete mechanical characterization: application to nanomet-

ric CrN/Cr multilayer coatings, *Appl. Phys.*, A 77, 419 – 426.

Mata, M., Alcalá, J., 2004, The role of friction on sharp indentation, *J. Mech. Physics of Solids*, 52, 145-165.

Matthews, A., Leyland, A., Holmberg, K., Ronkainen, H., 1998, Design aspects for advanced tribological surface coatings, *Surface Coatings Techn.*, 100-101, 1-6.

McHugh, P.E., Asaro, R.J., Shih, C.F., 1993, Computational modeling of metal matrix composite materials-I, Isothermal deformation patterns in ideal microstructures, *Acta Metallurgica*, 41, 1461-1476.

Mohammadi, S., Forouzan-Sepehr, S., Asadollahi, A., 2002, Contact based delamination and fracture analysis of composites, *Thin-Walled Structures*, 40, 595–609.

Morawiecki, M., Sadok, L., Wosiek, E., 1977, *Teoretyczne podstawy technologicznych procesów przeróbki plastycznej*, Śląsk, Katowice.

Nałęcz, M., 2001, *Sztuczne narządy*, Exit, Warszawa (in Polish).

Ning, Y., Polycarpou, A., Corny, T.F., 2004, Tip-radius effect in finite element modeling of sub-50 nm shallow nanoindentation, *Thin Solid Films*, 450, 295–303.

Ochelski, S., 2004, *Metody doświadczalne mechaniki kompozytów konstrukcyjnych*, WN-T, Warszawa (in Polish).

Oliver, C., Pharr, G.M., 1992, An improved technique for determining hardness and elastic modulus using load and displacement sensing indentation rxperiment, *J. Mater. Res.*, 7, 1564-1583.

Oleś, A., 1998, *Metody doświadczalne fizyki ciała stałego*, WN-T, Warszawa (in Polish).

Overview of Mechanical Testing Standards, 2002, Applications bulletin, CSM instruments, *Adv. Mech. Surface Testing*, 18.

http://www.csminstruments.com/frames/bullet/app18/appbull18.pdf

Panich, N., Sun, Y., 2004, Effect of penetration depth on indentation response of soft coatings on hard substrates: a finite element analysis, *Surface Coatings Techn.*, 182, 342-350.

Panich, N., Sun, Y., 2006, Mechanical characterization of nanostructured TiB$_2$ coatings using microscratch techniques, *Tribology Int.*, 39/2, 138-145.

Parameswaran, V., Shukla, A., 1998, Dynamic fracture of a functionally gradient material having discrete property variation, *J. Mater. Sci.*, 33, 3303-3311.

Paszyński, M., Kurtz, J. Demkowicz, L., 2006, Parallel fully automatic hp – adaptative 2D finite element package, *Comp. Meth. Appl. Mech. Eng.*, 195, 711-741.

Paszyński, M., Demkowicz, L., 2006, Parallel fully automatic hp – adaptative 3D finite element package*,* paper accepted to the special issue of *Engineering with Computers.*

Paszyński, M., Kopernik, M., Madej Ł., Pietrzyk, M., 2006, Automatic hp adaptivity to improve accuracy of modeling of heat transport and linear elasticity problems, *J. Machine Eng.*, 6, 73-82.

Pierce, D., Asaro, R.J., Needleman, A., 1983, Material rate dependence and localized deformation in crystalline solids, *Acta Metallurgica*, 31, 1951.

Pollini, I. Mosser, A., Parlebas, J.C., 2001, Electronic, spectroscopic and elastic properties of early transition metal compounds, *Physics Reports*, 355, 1–72.

Pompe, W., Worch, H., Epple, M., Friess, W., Gelinsky, M., Greil, P., Hempel, U., Scharnweber, D., Schulte, K., 2003, Functionally graded materials for biomedical applications, *Mat. Sci. Eng.*, A362, 40-60.

Prchlik, L., Pisacka, J., Sampath, S., 2003, Deformation and strain distribution in plasma sprayed nickel – aluminium coating loaded by spherical indenter, *Mat. Sci. Eng.*, A 360, 264-274.

Przygocki, W., Włochowicz, A., 2001, *Fizyka polimerów*, PWN, Warszawa.

Rauschenbach, B., Gerlach, J.W., 2000, Texture development in titanium nitride films grown by low-energy ion assisted deposition, *Cryst. Res. Technol.*, 35, 675–688.

Ravichandran, K.S., 1995, Thermal residual stresses in a Functionally Graded Material system, *Mat. Sci. Eng.*, A201, 269-276.

Saliklis, E.P., Urbanik, T.J., Tokyay, B., 2003, Bilinear Modeling of Cellulosic Orthotropic Nonlinear Materials, *J. Pulp and Paper Science*, 29/12, 407-411.

Santhanam, A.T., Quinto, D.T. Grab, G.P., 1996, Comparsion of the Steel-Millinig Performance of Carbide Inserts with MTCVD and PVD TiCN Coatings, *Int. J. Refractory Metals and Hard Materials*, 14, 31-40.

Schärer, S., Rohner, F., 2003, *Hardening steel nitriding*, Archieve Copy 2nd edition – Abridged, The Steelbands (Pan) of Trinidad and Tobago Archieves Database, http://www.seetobago.com/trinidad/pan/archieve/r&d/pan art/ir_archievecopy_hardening_steel_by_nitriding.htm.

Schwarzer, R.A., 2005, Advances in the analysis of texture and microstructure, *Arch. Metall. Mater.*, 50, 7-20.

Shouterden, K., Blanpain, B., Celis, J.P., Vingsbo, O., 1995, Fretting of titanium nitride and diamond-like carbon coatings at high frequencies and low temperature, *Wear*, 181-183, 86-93.

Szeliga, D., Pietrzyk, M., 2002, Identification of Rheological and Tribological Parameters, *Metal Forming Science and Practice, A State-of-the-art Volume in Honour of Professor J.A. Schey's 80th Birthday*, ed., Lenard J.G., Elsevier, Amsterdam, 227-258.

Stoney, G.G., 1909, The tension of metallic films deposited by electrolysis, *Proc. R. Soc. Lond.*, Ser. A82, 172-175.

Tabor, D., 1951, *The Hardness of metals*, Clarendon Press, London, 175.

Thogo, K., Sakaguchi, M., Ishii, H., 1996, Applicability of fracture mechanics in strength evaluation of functionally graded materials, *JSME Int. J. Series*, A 39, 479-488.

Thornton, J.A., 1974, Influence of apparatus geometry and deposition conditions on the structure and topography of thick sputtered coatings, *J. Vac. Sci. Technol.*, 11/4, 666-670.

Wang, H.F., Bangert, H., 1993, Three-dimensional finite element simulation of Vickers indentation on coated systems, *Mat. Sci. Eng.*, A163, 43-50.

Wu, P.-Q., Mohrbacher, H., Celis, J. P., 1996, The fretting behavior of PVD TiN coatings in aqueous solution, *Wear*, 201, 171-177.

Vieira, M.T., Ramos, A.S., 1999, The influence of ductile interlayers on the mechanical performance of tungsten nitride coatings, *J. Mat. Proc. Techn.*, 92-93, 156-161.

Volynskii, A.L., Bazhenov, S., Lebedeva, O.V., Ozerin, A.N., Bakeev, N.F., 1999, Multiple cracking of rigid platinum film covering polymer substrate, *J. Appl. Polymer Sci.*, 72/10, 1267.

Volynskii, A.L., Bazhenov, S., Lebedeva, O.V., Bakeev, N.F., 2000, Mechanical buckling instability of thin coatings deposited on soft polymer substrate, *J. Mat. Sci.,* 35, 547-554.

Yang, Z.M., Zhou, Z.G., Zhang, L.M., 2003, Characteristics of residual stress in Mo-Ti functionally graded material with continuous change in composition, *Mat. Sci. Eng.*, A359, 214-218.

E. Zoestbergen, 2000, *X-ray analysis of protective coatings*, http://dissertations.ub.rug.nl/FILES/faculties/science/2000/e.zoesterbergen/c5.pdf

OCENA MOŻLIWOŚCI PERSPEKTYWICZNYCH ZASTOSOWAŃ TWARDYCH NANO-POWŁOK

Streszczenie

Artykuł jest przeglądem badań nad zastosowaniem i metodami badań twardych nanopowłok. Metody otrzymywania tych materiałów oraz przykłady ich zastosowań są omówione w pierwszej części pracy. Dalsza część pracy dotyczy jej głównego celu, jakim jest numeryczne modelowanie odkształcania twardych nano powłok. Rozważono różne podejścia do tego problemu i omówiono podstawowe trudności pojawiające się w symulacji. Omówiono trzy podstawowe testy stosowane do identyfikacji własności analizowanych powłok. W końcowej części pracy opisano wykonane przez Autorów symulacje numeryczne i przedstawiono przykładowe wyniki dla testu wciskania wgłębnika w wielowarstwowy nanomateriał gradientowy. Analiza wyników potwierdza zdolność modelu MES do symulacji analizowanego procesu. Model ten zostanie wykorzystany w dalszych badaniach jako model zadania bezpośredniego w rozwiązaniu odwrotnym dla omawianych testów doświadczalnych.

COMPUTER METHODS IN MATERIALS SCIENCE